Hydrogen-Bonded Phosphate Esters. Synthesis and Structure of Imidazole-Containing Salts of Diphenyl Phosphate and (Trichloromethyl)phosphonic Acid

Robert R. Holmes,* Roberta O. Day, Yuji Yoshida,[1a] and Joan M. Holmes

Contribution from the Department of Chemistry, University of Massachusetts, Amherst, Massachusetts 01003. *Received February 11, 1991*

Abstract: Reaction of phosphorus acids with imidazole and 1-methylimidazole has led to the formation of the hydrogen-bonded salts, $[(PhO)_2PO_2][C_3H_3NHNMe]$ (**1**), $[(PhO)_2PO_2][C_3N_2H_5]$ (**2**), $[Cl_3CP(OH)O_2][C_3H_3NHNMe]\cdot H_2O$ (**3**), $[Cl_3CP(O-H)O_2][C_3N_2H_5]\cdot H_2O$ (**4**), and $[PhP(OH)O_2][C_3N_2H_5]$ (**5**). All were characterized by ^1H NMR and infrared spectroscopy. The X-ray structures of **1**–**4** were obtained. **1** forms as a hydrogen-bonded ion pair, and **2** forms hydrogen-bonded chains. **3** and **4** exist as monohydrates and form more complex networks, each possessing 12-membered hydrogen-bonded rings involving alternately water molecules and PO_2^- units of the phosphonate anion. ^1H NMR analyses of **1** and **5** indicate retention of the structures in solution, but on dilution a chain-like structure postulated for **5** is reasoned to break up into smaller units. A consequence of the study is an extension of the relation between the NH stretching frequency and N···O lengths in hydrogen-bonding compounds defining strong to intermediate hydrogen bonds useful in refining models for enzyme–substrate interactions. **1** crystallizes in the monoclinic space group $P2_1$, with $a = 7.929$ (2), $b = 11.353$ (3), $c = 9.066$ (1) Å, $\beta = 103.34$ (2)°, and $Z = 2$. **2** crystallizes in the triclinic space group $P\bar{1}$, with $a = 9.085$ (2), $b = 9.541$ (2), $c = 10.473$ (2) Å, $\alpha = 92.11$ (1)°, $\beta = 105.09$ (1)°, $\gamma = 115.10$ (1)°, and $Z = 2$. **3** crystallizes in the orthorhombic space group $Pbc2_1$, with $a = 8.866$ (1), $b = 13.510$ (2), $c = 20.404$ (4) Å, and $Z = 8$. **4** crystallizes in the monoclinic space group $P2_1/c$, with $a = 10.651$ (2), $b = 6.521$ (2), $c = 16.227$ (4) Å, $\beta = 95.41$ (2)°, and $Z = 4$. The final conventional unweighted residuals are 0.027 (**1**), 0.044 (**2**), 0.043 (**3**), and 0.048 (**4**).

Introduction

Hydrogen bonding is an important component of active site enzyme–substrate interactions involving phosphoryl-transfer reactions. A number of enzyme systems containing phosphorus substrates in place have been subjected to X-ray analysis and have led to the identification of major hydrogen-bonding interactions with active site residues, e.g., ribonuclease action on uridyl-(3′,5′)-adenosine[2,3] and staphylococcal nuclease action on thymidine 3′,5′-bis(phosphate).[4-9] However, a large degree of uncertainty exists in the magnitude of the resulting bond parameters, particularly those involving hydrogen bonds. More accurate structural parameters are available on simpler phosphate systems that incorporate a variety of hydrogen-bonding possibilities.[10-17] These studies not only provide useful information to refine the modeling of enzyme–substrate reactions[3,18-23] but have led to a degree of systemization of the number and type of interactions that occur.[17] Thus, O—O distances in P═O···H—O bonds and the O—N distances in P═O···H—N bonds show a general correlation increasing with a decrease in proton acidity.[17]

Some of the systems that have been studied by X-ray analysis[14,15,17] are depicted below, **A**–**D**, and illustrate the variety of hydrogen-bonding possibilities that have been identified. The superscripts associated with the formulas indicate references to the literature. Common among them are chain and dimer formulations.[10-17] A rationale for the appearance of these contrasting types of hydrogen-bonding systems has been presented in connection with our earlier work[17] on the catechol-containing salts of 2-hydroxyphenyl phenylphosphonate, **A** and **B**.

In the present paper, we examine the ability of imidazole and methylimidazole to form hydrogen bonds with the phosphorus acids, $(PhO)_2PO(OH)$, $Cl_3CPO(OH)_2$, and $PhPO(OH)_2$. These important active site bases provide two N–H and one N–H groups, respectively. The work resulted in the synthesis and ^1H NMR, infrared, and X-ray studies of $[(PhO)_2PO_2][C_3H_3NMeNH]$ (**1**), $[(PhO)_2PO_2][C_3N_2H_5]$ (**2**), $[Cl_3CP(OH)O_2][C_3H_3NMeNH]\cdot H_2O$ (**3**), and $[Cl_3CP(OH)O_2][C_3N_2H_5]\cdot H_2O$ (**4**). In addition, the synthesis and ^1H NMR and infrared characterizations of $[PhP(OH)O_2][C_3N_2H_5]$ (**5**) were carried out. The study was undertaken to determine the extent and type of hydrogen bond

(1) (a) This work represents a portion of the M.S. Thesis of Yuji Yoshida, University of Massachusetts, Amherst, MA. (b) Presented at the 6th International Symposium on Inorganic Ring Systems (IRIS VI), August 18–22, 1991, Berlin, Germany.

(2) Richards, F. M.; Wyckoff, H. W. *Atlas of Molecular Structures in Biology*; Phillips, D. C., Richards, F. M., Eds.; Clarendon Press: Oxford, 1973; Vol. 1.

(3) Holmes, R. R.; Deiters, J. A.; Gallucci, J. C. *J. Am. Chem. Soc.* **1978**, *100*, 7393.

(4) Anfinsen, C. B.; Cuatrecasas, P.; Taniuchi, H. *The Enzymes*, 3rd ed.; Boyer, P. D.; Ed.; Academic Press: New York, 1971; Vol. IV, pp 177–204.

(5) (a) Cotton, F. A.; Day, V. W.; Hazen, E. E., Jr.; Larsen, S. *J. Am. Chem. Soc.* **1973**, *95*, 4834. (b) Cotton, F. A.; Hazen, E. E., Jr.; Legg, M. J. *Proc. Natl. Acad. Sci. U.S.A.* **1979**, *76*, 2551.

(6) Arnone, A.; Bier, C. J.; Cotton, F. A.; Day, V. W.; Hazen, E. E., Jr.; Richardson, D. C.; Richardson, J. S.; Yonath, A. *J. Biol. Chem.* **1971**, *246*, 2302.

(7) Arnone, A.; Bier, C. J.; Cotton, F. A.; Hazen, E. E., Jr.; Richardson, D. C.; Richardson, J. S. *Proc. Natl. Acad. Sci. U.S.A.* **1969**, *64*, 420.

(8) Trueblood, K. N.; Horn, P.; Luzzati, V. *Acta Crystallogr., Sect. B* **1961**, *14*, 965.

(9) Young, D. W.; Tollin, P.; Wilson, H. R. *Acta Crystallogr., Sect. B* **1969**, *25*, 1423.

(10) Tkachev, V. V.; Atovmyan, L. O.; Kardanov, N. A.; Godovikov, N.; Kabachnik, M. I. *Zh. Strukt. Khim.* **1978**, *19*, 962.

(11) Antipin, M. Yu.; Struchkov, Yu. T.; Matrosov, E. I.; Bondarenko, N. A.; Tsvetkov, E. N.; Kabachnik, M. I. *Zh. Strukt. Khim.* **1981**, *22*, 100.

(12) Wieczorek, M. W.; Karolak-Wojciechowska, J.; Mikolajczyk, M.; Witczak, M. *Acta Crystallogr., Sect. B* **1978**, *B34*, 3138.

(13) du Plessis, M. P.; Modro, T. A.; Nassimbeni, L. R. *Acta Crystallogr., Sect. B* **1982**, *B38*, 1504.

(14) Sundaralingam, M.; Harmony, T. P.; Prusiner, P. *Acta Crystallogr., Sect. B* **1982**, *B38*, 1536.

(15) Varughese, K. I.; Lu, C. T.; Kartha, G. *J. Am. Chem. Soc.* **1982**, *104*, 3398.

(16) Brianso, M.-C.; Surcouf, E. *Acta Crystallogr., Sect. B* **1978**, *B34*, 681.

(17) Poutasse, C. A.; Day, R. O.; Holmes, R. R. *J. Am. Chem. Soc.* **1984**, *106*, 3814.

(18) Mildvan, A. S. *Annu. Rev. Biochem.* **1974**, *43*, 357.

(19) For a more extensive coverage than ref 4, see: Holmes, R. R. *Pentacoordinated Phosphorus*; American Chemical Society: Washington, DC, 1980; Vol. II, ACS Monogr. No. 176.

(20) Deiters, J. A.; Gallucci, J. C.; Clark, T. E.; Holmes, R. R. *J. Am. Chem. Soc.* **1977**, *99*, 5461.

(21) Deiters, J. A.; Gallucci, J. C.; Holmes, R. R. *J. Am. Chem. Soc.* **1982**, *104*, 5457.

(22) Deiters, J. A.; Holmes, R. R. *J. Am. Chem. Soc.* **1983**, *105*, 609.

(23) Deiters, J. A.; Holmes, R. R. *J. Am. Chem. Soc.* **1984**, *106*, 3307 and references cited therein.

0002-7863/92/1514-1771$03.00/0 © 1992 American Chemical Society

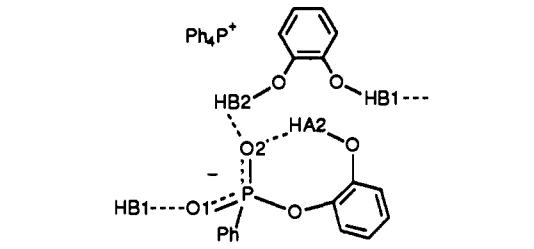

A[17]

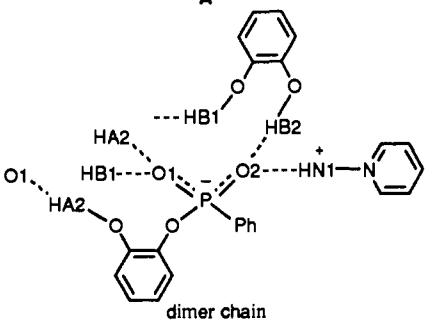

B[17]

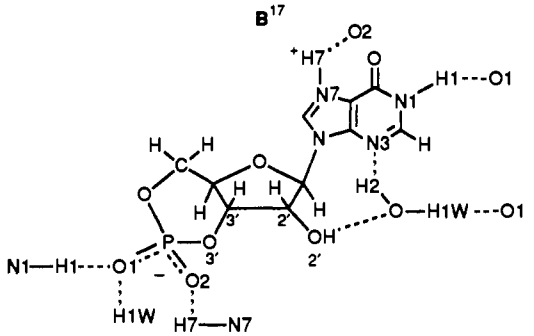

Zwitterionic Inosine Cyclic 3',5'-Monophosphate (CIMP)

C[14] polymer network

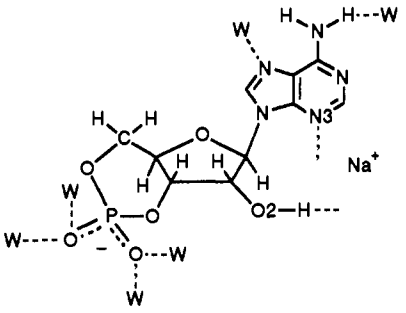

Cyclic Adenosine 3',5'-Monophosphate Sodium Salt Tetrahydrate

D[15] dimer (W = water)

interactions that occur between these bases and phosphoryl groups in a variety of formulations and to extend a relation between the NH stretching frequency and N–H···O hydrogen bond lengths defining strong to intermediate hydrogen bonds, which should prove useful in model studies of enzyme–substrate interactions.

Results

X-ray Studies. The atom labeling schemes for **1–4** are given in the ORTEP plots of Figures 1–4, respectively. Selected bond lengths and angles for **1** and **2** are given in Table I, while corresponding data for **3** and **4** are presented in Table II. Figure 5 is an ORTEP plot showing the extensive hydrogen-bonding network for **4**. Figure 3 is a similar plot for **3**. Specific hydrogen bond interactions are summarized in Table III for **1–4**. For all four compounds, atomic coordinates, refined hydrogen atom parameters, anisotropic thermal parameters, calculated hydrogen atom parameters, and additional bond lengths and angles are provided as supplementary material.

NMR and IR Studies. The results of dilution studies on proton chemical shifts in DMSO-d_6 for the imidazolium salt of phenylphosphonic acid (**5**) are summarized in Table IV. The results of a similar NMR dilution study for the 1-methylimidazolium salt of diphenyl phosphate (**1**) are listed in Table V. Infrared N–H

Table I. Selected Bond Lengths (Å) and Angles (deg) in Crystalline $[(PhO)_2PO_2][C_3H_3NHNMe]$ (**1**) and $[(PhO)_2PO_2][C_3N_2H_5]$ (**2**)[a]

Length

compd[b]	1	2	compd[b]	1	2
P–O1	1.618 (2)	1.602 (2)	O1–C11	1.387 (3)	1.395 (3)
P–O2	1.623 (2)	1.609 (2)	O2–C21	1.390 (3)	1.408 (3)
P–O3	1.465 (2)	1.479 (2)	N3–H3	0.71 (4)	0.90 (4)
P–O4	1.485 (2)	1.478 (2)	N1–H1		0.79 (4)

Angle

compd	1	2
O1–P–O2	103.1 (1)	100.7 (1)
O1–P–O3	110.7 (1)	110.0 (1)
O1–P–O4	104.4 (1)	108.9 (1)
O2–P–O3	105.2 (1)	111.0 (1)
O2–P–O4	109.2 (1)	105.4 (1)
O3–P–O4	122.7 (2)	119.2 (1)
P–O1–C11	120.4 (1)	123.6 (2)
P–O2–C21	125.0 (1)	120.0 (1)
P–O3–H1		133 (1)
P–O4–H4	144 (1)	130 (1)
O1–C11–C12	119.5 (2)	121.1 (3)
O1–C11–C16	119.9 (2)	117.5 (3)
O2–C21–C22	122.6 (2)	119.6 (3)
O2–C21–C26	116.3 (2)	119.1 (3)
H1–N1–C2		127 (3)
H1–N1–C5		124 (3)
H3–N3–C2	124 (4)	122 (2)
H3–N3–C4	128 (3)	129 (2)

[a] Numbers in parentheses are estimated standard deviations. [b] Atoms are labeled to agree with Figures 1 and 2.

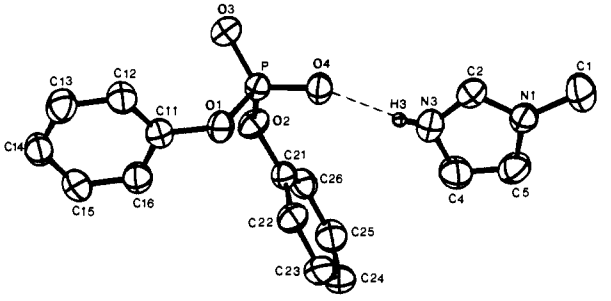

Figure 1. ORTEP plot of $[(PhO)_2PO_2][C_3H_3NMeNH]$ (**1**) with thermal ellipsoids at the 50% probability level. Hydrogen atoms, except for H3 which is represented by a sphere of arbitrary radius, are omitted for purposes of clarity. The hydrogen-bonding interaction is shown as a dashed line.

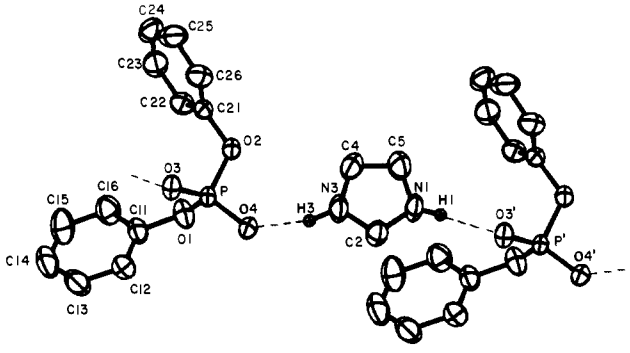

Figure 2. ORTEP plot of $[(PhO)_2PO_2][C_3N_2H_5]$ (**2**) with thermal ellipsoids at the 50% probability level. A translationally-related anion is included ($' = x, 1 + y, z$) to show the propagation of the hydrogen-bonded chain. Hydrogen atoms, except for H1 and H3 which are shown as spheres of arbitrary radii, are omitted for purposes of clarity. Hydrogen-bonding interactions are shown as dashed lines.

Table II. Selected Bond Lengths (Å) and Angles (deg) in Crystalline $[Cl_3CP(OH)O_2][C_3H_3NHNMe]\cdot H_2O$ (**3**) and $[Cl_3CP(OH)O_2][C_3N_2H_5]\cdot H_2O$ (**4**)[a]

Length

	3		
compd[b]	X = A	X = B	4
PX–OX1	1.492 (7)	1.498 (7)	1.561 (3)
PX–OX2	1.559 (6)	1.557 (6)	1.490 (3)
PX–OX3	1.483 (6)	1.472 (6)	1.482 (3)
PX–CX1	1.87 (2)	1.86 (1)	1.854 (5)

Angle

	3		
compd	X = A	X = B	4
OX1–PX–OX2	108.5 (4)	107.6 (4)	109.8 (2)
OX1–PX–OX3	120.1 (4)	119.8 (4)	112.5 (2)
OX1–PX–CX1	105.6 (6)	106.3 (6)	102.5 (2)
OX2–PX–OX3	113.5 (4)	113.5 (3)	118.5 (2)
OX2–PX–CX1	101.8 (4)	102.3 (4)	105.9 (2)
OX3–PX–CX1	105.4 (4)	105.5 (4)	106.0 (2)

[a] Numbers in parentheses are estimated standard deviations. [b] Atoms are labeled to agree with Figures 3 and 4.

stretching frequencies for **1–5** as halocarbon grease mulls are reported in Table VI.

Discussion

Synthesis. Imidazolium phosphates and phosphonates were prepared by reaction of equimolar portions of the acid and base components in dichloromethane at room temperature. Equation 1 illustrates the reaction for the formation of **1**. Although

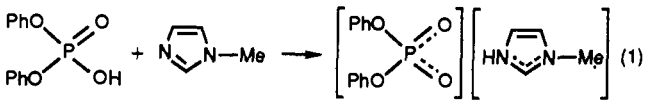

(1)

1

phosphate **1** was very hygroscopic, elemental analysis and the X-ray study corresponded to an anhydrous substance, whereas the phosphonates **3** and **4** formed as monohydrates, as revealed in the X-ray analysis. Water could be removed in vacuo, but crystallinity was reduced sufficiently to disallow an X-ray analysis of the anhydrous salts.

Hydrogen Bonding. Hydrogen bonding provides a lattice for **1** which consists of a hydrogen-bonded ion pair, while **2** has a chain structure. For the hydrated phosphonate salts, **3** and **4**, more complex arrays are obtained. Both have rings with alternate phosphonate and water molecules hydrogen bonded to each other giving 12-membered rings. Due to the presence of the water molecules, **3** and **4** also have two-dimensional hydrogen-bonded networks in common. In all four structures, every NH or OH hydrogen atom is involved in a single hydrogen bond to an acceptor oxygen atom.

In **1**, the single donor group N3–H3 (Figure 1) forms a hydrogen bond to the phosphoryl oxygen atom, O4, resulting in a lattice composed of hydrogen-bonded anion–cation dimers. This salt is the lowest melting of the four, which is consistent with the absence of hydrogen-bonded chains or networks. The very hygroscopic nature of the crystals may reflect the ability of the non-hydrogen-bonded phosphoryl oxygen atom, O3, to form hydrogen bonds with water.

In **2**, there is an NH group present for each phosphoryl oxygen atom, resulting in two independent hydrogen-bonding interactions. Each cation is positioned between a pair of translationally related anions (or alternatively each anion is positioned between a pair of translationally related cations), forming hydrogen-bonded chains along the $\vec{b}$ direction of the lattice (Figure 2).

Compounds **3** and **4** are both monohydrates in which each water molecule is involved in two donor interactions, forming a bridge between phosphoryl oxygen atoms of two anions, and one acceptor interaction with the OH group of a third anion. Another common structural feature in **3** and **4** is the presence of 12-membered hydrogen-bonded rings. In **3** the sequence is O–P–O···H–O–H···O–P–O···H–O–H with only water hydrogen atoms involved. In **4** the hydroxyl group of an anion is involved: O–P–O···H–O–H···O–P–O–H···O–H.

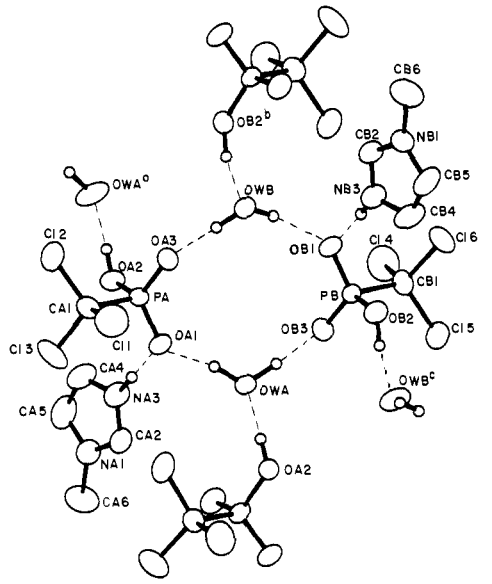

Figure 3. ORTEP plot of $[Cl_3CP(OH)O_2][C_3H_3NHNMe]\cdot H_2O$ (**3**) with thermal ellipsoids at the 50% probability level. A pair of symmetry-related water molecules ($a = 1 - x, y - {}^1/_2, z$; $c = x, {}^1/_2 + y, z$) and a pair of symmetry-related anions ($b = x, y - {}^1/_2, z$; $d = 1 - x, {}^1/_2 + y, z$) are included to illustrate the hydrogen-bonding interactions. Hydrogen atoms, except for those involved in hydrogen bonds which are represented as spheres of arbitrary radii, are omitted for purposes of clarity. Hydrogen bonds are shown as dashed lines.

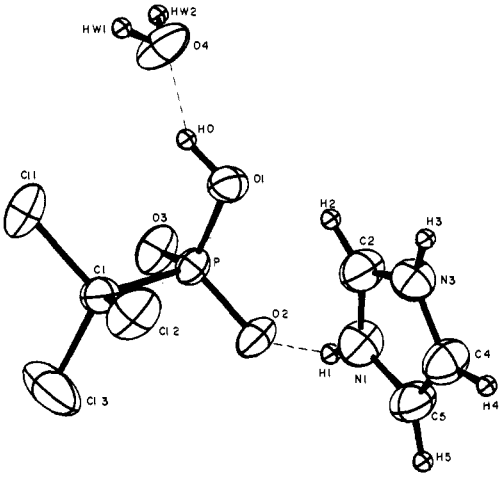

Figure 4. ORTEP plot of $[Cl_3CP(OH)O_2][C_3N_2H_5\cdot H_2O$ (**4**) with thermal ellipsoids at the 50% probability level. Hydrogen atoms are represented by spheres of arbitrary radii. Hydrogen bonds within the asymmetric unit are shown as dashed lines.

In **3**, the asymmetric unit consists of two independent cation, anion, water groupings (labeled A and B in Figure 3) which are roughly related by a non-crystallographic inversion center at (1/**4**, 3/8, 1/2) and form the aforementioned 12-membered hydrogen-bonded ring. The two independent cations of the asymmetric unit are pendant from this 12-membered ring as a result of N–H···O hydrogen bonds to phosphoryl oxygen atoms. Pairs of translationally-related and screw-related units along $\vec{a}$ and $\vec{b}$ are joined by hydrogen bonds between the hydrogen atoms of the hydroxyl groups of the cations and the oxygen atoms of the water molecules, forming a two-dimensional hydrogen-bonded network.

In **4** the asymmetrical unit is a single anion, cation, water grouping in which the anion is hydrogen bonded to the cation via a phosphoryl oxygen atom (O2···H1–N1, Figure 4) and to the oxygen atom of the water molecule via its hydroxyl group (O1–

Table III. Bond Parameters for Hydrogen-Bonded Phosphoryl Groups

entry[a]	bond distance, Å[b]	A···O,[c] Å	A–H···O angle, deg	H-bond type	no. of atoms per ring/ no. of H bonds
1_1	O3 ····· P ····· O4 ····· H3 —— N3 1.465(2) 1.485(2) 1.95(4) 0.71(4)	2.650 (3)	169 (4)	ion pair	
2_1	O3 ····· P ····· O4 ····· H3 —— N3 1.479(2) 1.478(2) 1.78(4) 0.90(4)	2.647 (3)	162 (4)	intermolecular chain	
2_2	O4 ····· P ····· O3 ····· H1 —— N1 1.478(2) 1.479(2) 1.88(4) 0.79(4)	2.669 (4)	173 (4)	intermolecular chain	
$3A_1$[d]	OA1 ····· PA ····· OA3 ····· HWB1 —— OWB 1.492(7) 1.483(6) 1.66 1.01	2.673 (7)	180	intermolecular ring	12/4
$3A_2$	OA3 ····· PA ····· OA1 ····· HWA1 —— OWA 1.483(6) 1.492(7) 1.68 1.06	2.729 (7)	171	intermolecular ring	12/4
$3A_3$	OA3 ····· PA ····· OA1 ····· HNA3 —— NA3 1.483(6) 1.492(7) 1.76 0.99	2.751 (7)	177	intermolecular ion pair	
$3B_1$[d]	OB1 ····· PB ····· OB3 ····· HWA2 —— OWA 1.498(7) 1.472(6) 1.65 1.05	2.690 (7)	172	intermolecular ring	
$3B_2$	OB3 ····· PB ····· OB1 ····· HWB2 —— OWB 1.472(6) 1.498(7) 1.84 0.94	2.731 (7)	158	intermolecular ring	
$3B_3$	OB3 ····· PB ····· OB1 ····· HNB3 —— NB3 1.472(6) 1.498(7) 1.71 1.01	2.706 (9)	170	ion pair	
4_1	O3 ····· P ····· O2 ····· H1 —— N1 1.482(3) 1.490(3) 1.87 0.90	2.737 (4)	161	intermolecular chain	
4_2	O3 ····· P ····· O2 ····· HW1 —— O4 1.482(3) 1.490(3) 1.83 0.93	2.716 (4)	157	intermolecular ring	12/4
4_3	O2 ····· P ····· O3 ····· H3 —— N3 1.490(3) 1.482(3) 1.92 0.90	2.755 (4)	154	intermolecular chain	
4_4	O2 ····· P ····· O3 ····· HW2 —— O4 1.490(3) 1.482(3) 1.79 0.91	2.688 (4)	166	intermolecular ring	12/4
$3A_4$[e]	P —— OA2 —— HOA2 ····· OWA 1.559(6) 0.926 1.644	2.569 (7)	178	intermolecular chain	
$3B_4$[e]	PB —— OB2 —— HOB2 ····· OWB 1.557(6) 1.013 1.581	2.564 (7)	162	intermolecular chain	
4_5[e]	P —— O1 —— HO ····· O4 1.561(3) 0.957 1.701	2.560 (4)	148	intermolecular ring	

[a] The subscript numbers are used only to refer to different entries for the same molecule. [b] The PO_2 unit has a negative charge. [c] A is the non-hydrogen atom (O or N) involved in the hydrogen bond interaction. [d] Two independent molecular assemblies per unit cell labeled A and B in Figure 3. [e] Bond parameters for hydrogen-bonded P–OH groups.

HO···O4). Translationally related groupings along $\vec{b}$ form a hydrogen-bonded chain due to a second hydrogen-bonding interaction between the phosphoryl oxygen atoms O2 and the hydrogen atoms HW1 of the water molecules (Figure 5). In addition to the chains along $\vec{b}$, there are hydrogen-bonded chains along $\vec{c}$ due to interactions with *c*-glide-related units (N3–H3···O3). Thus there is a two-dimensional hydrogen-bonded network. Pairs of these networks are joined by the aforementioned 12-membered rings due to interactions with 2_1 screw-related units (O4–HW2···O3). In Figure 5 only one such 12-membered ring is shown, for purposes of clarity.

It is interesting to note that in **3** only one of the two phosphoryl oxygen atoms is involved in two hydrogen bonds, while in **4** both of the phosphoryl oxygen atoms are involved in two hydrogen bonds. This observation is consistent with the fact that in **4** there is an extra hydrogen-bonding site in the cation.

The formation of 12-membered rings in **3** and **4** is reasonable between PO_2 phosphoryl units and H_2O molecules since a minimum of two each of these entities is required to form a ring. Less easy to rationalize is the difference in ring composition between **3** and **4**. Both hydrogen atoms of the water molecules participate in hydrogen bond ring formation in **3**, whereas for **4** only one of the hydrogens of each water molecule is involved in ring formation. The difference in ring components is made up in **4** by inclusion of the OH group of one of the phosphonate anions.

Hydrogen Bond Parameters. Table III summarizes hydrogen bond parameters useful for comparisons with similar data for the related phosphorus compounds, A–D,[14,15,17] displayed in the Introduction as well as others not displayed.[10-13] The shortest O···N length reported so far for the O···H–N hydrogen bond system is found in **B**[17] between the phosphonate O2 atom and pyridinium ion N atom at 2.600 (5) Å. The O···H–N hydrogen bond in **B** approaches linearity at 172 (5)°. A similar short O···N distance for the O···H–N hydrogen bond has been reported in 1,2,3-benzotriazolium dihydrogen phosphate, $[C_6H_4N_3H_2][H_2PO_4]$ (**E**).[24] The O1–N3 distance is 2.611 Å; however, no angle was given.[25]

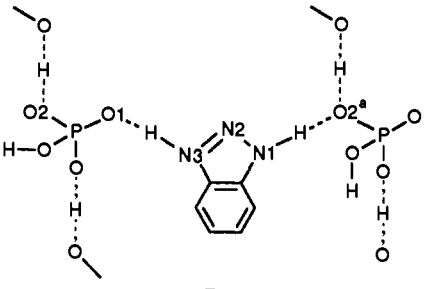

E

The most significant comparison among the hydrogen bond parameters listed in Table III is found in the relative values of the A···O distances (for A = N). The average value of the N···O distance for the diphenyl phosphates **1** and **2** is 2.65 Å, whereas that for the phosphonates **3** and **4** is 2.74 Å. The average N–H···O angle is 165.5° for **1** and **2**, which is the same for **3** and **4**. This lengthening most likely reflects the greater number of hydrogen

(24) Emsley, J.; Reza, N. M.; Dawes, H. M.; Hursthouse, M. B. *J. Chem. Soc., Chem. Commun.* **1985**, 1458.

(25) A recent book (Jeffrey, G. A.; Saenger, W. *Hydrogen Bonding in Biological Structures*; Springer-Verlag: New York, 1991) provides a detailed discussion of a basis for comparing lengths of hydrogen bonds using "normalized" H–N distances in the absence of neutron data. We choose not to use the latter approach since most of the hydrogen-bonding literature we are focusing on includes the non-hydrogen atom separation, which is of interest to the practicing inorganic chemist.

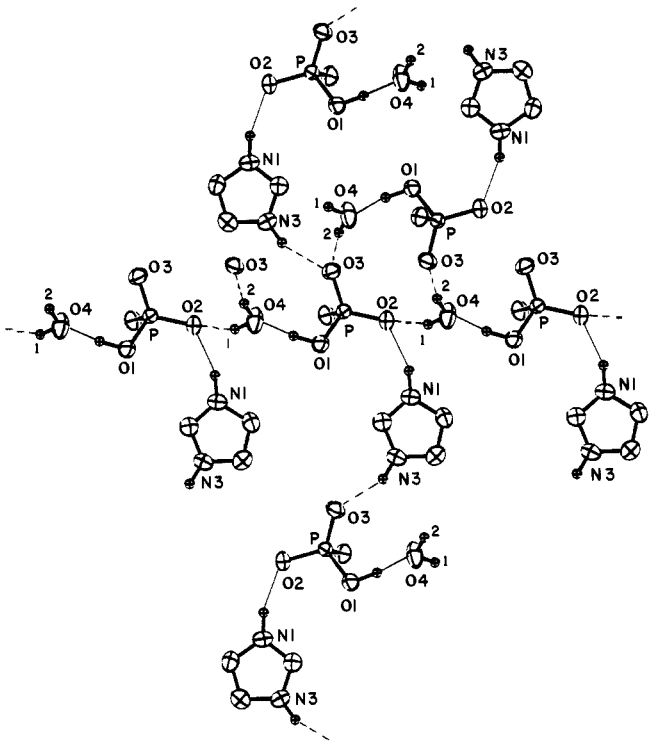

Figure 5. ORTEP plot of **4**, viewed normal to the *b,c* plane, showing the propagation of the two-dimensional hydrogen-bonded network. The asymmetric unit plus five symmetry-related units are shown. Intraunit hydrogen bonds are shown as narrow solid lines, while interunit bonds are shown as dashed lines. The chlorine atoms and hydrogen atoms which are not involved in hydrogen bonds have been omitted for purposes of clarity. An additional symmetry-related O3 is shown to complete the illustration of the hydrogen-bonding interactions in the asymmetric unit.

bonds in the more complex hydrated networks **3** and **4**. Each phosphoryl oxygen atom in these structures has two hydrogen bonds, which would tend to reduce their individual strengths compared to that in the phosphate salts **1** and **2** that contain a maximum of one hydrogen bond per P–O oxygen linkage. As already pointed out, one of the P–O bonds in **1** is not involved in any hydrogen bonding.

The charge on the nitrogen system also has an effect on the N···O distances. All of the imidazole derivatives in this study have a positive charge. Comparison of **1** and **2** with **F** and **G**, all of which have one hydrogen bond per phosphoryl oxygen, shows an increase in the O···N distance from 2.66 (average value for **1** and **2**) to 2.85 Å (average value for **F** and **G**), an even greater effect than that produced when going from one to two hydrogen bonds per phosphoryl oxygen. The charge and complexity of the hydrogen-bonding system represent two of the most important factors to evaluate in constructing active site models of phosphoryl-transfer enzymes.

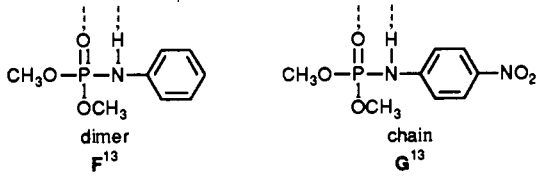

dimer
F^{13}

chain
G^{13}

The use of accurate hydrogen bond parameters in defining enzyme–substrate interactions is of value in both modeling studies employing a molecular mechanics approach and in X-ray refinement of protein structures. These two kinds of studies have depended on the availability of accurate values from small-molecule studies; for example, their use was employed in the computer simulation[21,22] of an active site model of the intermediate formed in enzymatic hydrolysis of (*p*-nitrophenyl)deoxythymidine diphosphate, *p*-NO_2Ph-pdTp, by staphylococcal nuclease. Recent X-ray work by Loll and Lattman[26] indicates the degree presently

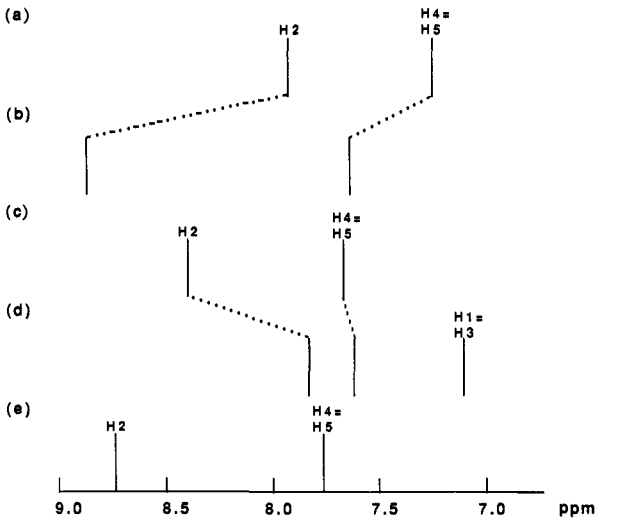

Figure 6. Display of proton chemical shifts (ppm) of (a) imidazole in 10% DMSO-d_6;[27] (b) imidazolium trifluorocarboxylate, $[C_3N_2H_5][CF_3CO_2]$, in CF_3CO_2H;[27] (c) $[PhP(OH)O_2][C_3N_2H_5$ (**5**) in DMSO-d_6 at 0.216 M; (d) at 0.005 M; and (e) at 0.216 M to which D_2O has been added.

reached in structural refinement of staphylococcal nuclease.

^{1}H NMR. Proton NMR dilution studies confirm the presence of hydrogen bonding in solution between imidazolium cations and phosphate anions. One such study was conducted on the imidazolium salt of phenylphosphonic acid (**5**), in DMSO-d_6, and a second on the 1-methylimidazolium salt of diphenyl phosphate (**1**). The proton numbering scheme is given here.

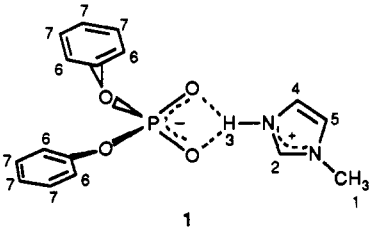

1

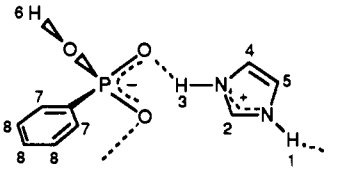

5

In contrast to the X-ray structure of **1** (Figure 1), both phosphoryl oxygen atoms are shown hydrogen bonded to methylimidazole.

As discussed in the literature, ^{1}H NMR signals assigned to the various protons for the neutral imidazole molecule, Figure 6a, and 1-methylimidazole, Figure 7a, are shown to shift downfield on formation of the imidazolium salts with CF_3CO_2H, Figures 6b and 7b, respectively.[27] The greater downfield shift for H2 compared to H4 and H5 is rationalized by the greater positive charge residing on H2 in the hydrogen-bonded imidazolium cation.[27] Similarly, for **5** and **1** in DMSO-d_6 and $CDCl_3$ solutions, Figures 6c and 7c, respectively, and corresponding data in Tables IV and V, the ^{1}H NMR signal assigned to H2 shows the greatest downfield shift. Although the signal assigned to H4 and H5 for **5** shifts downfield on salt formation (cf. Figure 6a,c), a slight upfield shift is apparent for the signal of the H4 proton of **1** while the signal for H5 hardly changes at all (cf. Figure 7a,c). It is possible that shielding of H4 and H5 by the phenyl groups in the hydrogen-bonded ion pairs of **1** counteracts the effect of the increase in positive charge felt on imidazolium ion formation. For

(26) Loll, P. J.; Lattman, E. E. *Proteins: Struct., Funct., Genet.* **1989**, *51*, 183.

(27) Barlin, G. B.; Batterham, T. J. *J. Chem. Soc. B* **1967**, 516.

Table IV. Dilution Study of Proton Chemical Shifts of **5** in DMSO-d_6 (ppm)

compd	conc (M)	H-1	H-2	H-3	H-4	H-5	H-7	H-8	ref
Im[a]			7.92		7.25	7.25			27
$ImH^+CF_3CO_2^-$[b]			8.82		7.66	7.66			27
$PhP(O)(OH)_2$							7.63–7.74	7.50	this work
5[c]	0.216	*d*	8.40	*d*	7.73[e]	7.73[e]	7.36	7.36	this work
5[c]	0.108	6.89	8.29	6.89	7.67	7.67	7.39	7.36	this work
5[c]	0.054	7.37	8.29	7.37	7.77	7.77	7.49	7.47	this work
5[c]	0.027	7.28	8.13	7.28	7.71	7.71	7.46	7.43	this work
5[c]	0.005	7.10	7.84	7.10	7.65	7.65	7.42	7.38	this work
5[c]	0.216[f]		8.76		7.80	7.80	7.56	7.55	this work
5[c]	0.108[f]		8.68		7.70	7.70	7.47	7.44	this work

[a] Imidazole in 10% DMSO-d_6 solution. [b] Imidazolium$^+$ $CF_3CO_2^-$ in CF_3CO_2H. [c] No signal was identified for H-6, presumably due to rapid exchange. The H-7 and H-8 signals may be interchanged since the integrated intensities were not significantly different. [d] No signal, presumably due to rapid exchange. The H-1 and H-3 signals for more dilute concentrations were relatively broad singlets. [e] H-4 = H-5 signals showed quartet patterns. [f] Addition of D_2O to these solutions caused the disappearance of the signals for H-1 and H-3, presumably due to rapid chemical exchange.

Table V. Dilution Study of Proton Chemical Shifts of **1** in $CDCl_3$ (ppm)

compd	conc (M)	H-1	H-2	H-3	H-4	H-5	H-6 (or H-7)	H-7 (or H-6)	ref
1-MIm[a]		3.70	7.47		7.08	6.88			27
1-$MImH^+CF_3CO_2^-$[b]		4.11	8.73		7.60	7.52			27
1	0.253	3.68	8.81	7.03	6.97	6.89	7.25	7.22	this work
1	0.126	3.72	8.87	7.26	7.02	6.94	7.26	7.23	this work
1	0.063	3.74	8.90	*c*	*c*	6.95	7.27	7.24	this work
1	0.031	3.76	8.88	*c*	*c*	6.95	7.27	7.24	this work
1	0.0080	3.81	8.69	*c*	*c*	7.05	7.29	7.25	this work

[a] 1-Methylimidazole in 10% $CDCl_3$ solution. [b] 1-Methylimidazolium$^+$ $CF_3CO_2^-$ in CF_3CO_2H. [c] Not determined because of mixing of the H-3 and H-4 signals.

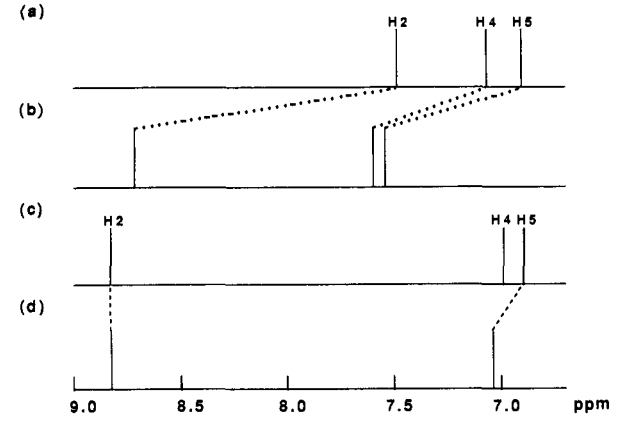

Figure 7. Display of proton chemical shifts (ppm) of (a) 1-methylimidazole in 10% $CDCl_3$ solution;[27] (b) 1-methylimidazolium trifluorocarboxylate, $[C_3H_3NMeNH][CF_3CO_2]$, in CF_3CO_2H;[27] (c) $[(PhO)_2PO_2][C_3H_3NMeNH]$ (**1**) in $CDCl_3$ at 0.253 M; and (d) at 0.031 M.

5 in a hydrogen-bonded polymeric form, the latter shielding might be more effective at H2 than H4 or H5 to account for its greater upfield signal compared to that in CF_3CO_2H (Figure 6b).[28,29] Addition of D_2O to the DMSO-d_6 solution of Figure 6c causes downfield shifts of all protons (cf. Figure 6e), which is indicative of enhanced hydrogen bond formation with D_2O and the break-up of the hydrogen-bonded network with the anion of phenylphosphonic acid.

Dilution of the 0.216 M solution of **5** (Figure 6c), to 0.006 M (Figure 6d) results in upfield shifts consistent with the disruption of the one-dimensional polymeric hydrogen-bonded network that is postulated to be present. The existence of the latter network in solution also is reasonable on the basis of solid-state X-ray study of **2** establishing this type of structure. Also consistent with the X-ray study of **1** establishing hydrogen-bonded ion pairs is the dilution of the 0.253 M $CDCl_3$ solution of Figure 7c to 0.031 M (Figure 7d), which shows little change in the chemical shifts of H2 or H5. The ion pairs appear to remain as such. Additional ^1H NMR data and assignments are listed in Tables IV and V.

The assignments for the various protons in **1** and **5** were aided by analogies with the ^1H NMR work of Barlin and Batterham[27] on the neutral imidazoles and their salts in CF_3CO_2H (cf. Figures 6a,b and 7a,b). The signals for H1 and H3 of **5** were verified by the addition of D_2O (Figure 6e), which caused their disappearance (cf. with Figure 6d and dilution data of Table IV). The onset of rapid exchange of these labile protons in the presence of D_2O is believed responsible for the loss of the H1 and H3 signals. Signal assignments in general agree with integrated intensities and splitting patterns where resolvable. Thus with **5**, a quartet results for H4 (=H5), e.g., H4 split by H5 and H3.

Table VI. N–H Stretching Frequency vs N···O Length for Compounds **1–5** Containing the N–H···O Hydrogen Bond

compd[a]	N···O, Å[b]	ν_{NH}, cm^{-1}
4	2.746	2580
3	2.729	2320
2	2.658	2460
1	2.650	2320
5		2320

[a] This work. Infrared spectra of halocarbon grease mulls. [b] Average values.

Table VII. Effect of Hydrogen Bond Formation on the Phosphoryl Stretching Frequency (cm^{-1})[a]

acid	ν_1(P=O)	salt	ν_2(P···O)	$\nu_1 - \nu_2$
$PhP(O)(OH)_2$	1140 (s)	**5**	1080 (s)	60
$Cl_3CP(O)(OH)_2$	1060 (s)	**4**	945 (m)	115
$Cl_3CP(O)(OH)_2$	1060 (s)	**3**	938 (m)	122
$(PhO)_2P(O)OH$	1178 (s)	**1**	1080 (s)	98

[a] Nujol mulls.

Infrared. The phosphorus acids used in this study are capable of forming intermolecular O–H···O hydrogen bonds via a dimer formulation.[30] Infrared absorptions appear as broad peaks

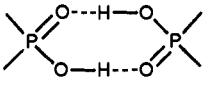

(28) Shielding effects in aromatic solvents have been discussed in these terms in ref 27. See also ref 29.

(29) Bhacca, N. S.; Williams, D. H. *Applications of NMR Spectroscopy in Organic Chemistry*; Holden-Day: San Francisco, 1964; p 159.

(30) Burg, A. B.; Griffiths, J. E. *J. Am. Chem. Soc.* **1961**, *83*, 4333.

overlapping each other at 2700 (s) and 2260 (s) cm^{-1} for phenylphosphonic acid, at 2700 (s) and 2250 (s) cm^{-1} for (trichloromethyl)phosphonic acid, and at 2700 (s) and 2280 (s) cm^{-1} for diphenyl phosphate. On salt formation with the imidazoles, these bands disappear or are shifted, and new broad bands associated with N–H stretching modes appear. NH bands that are likely to be associated with hydrogen-bonded N–H···O stretching modes are listed in Table VI, while phosphoryl stretching frequencies for the acids and imidazole salts, **1** and **3–5**, are compared in Table VII. The latter phosphoryl frequencies are lowered by 60–122 cm^{-1} on formation of the salts, consistent with an expected reduced bond order associated with the P–O linkages. In agreement, the P–O3 bond length involving this non-hydrogen-bonded oxygen atom is 1.465 (2) Å, which is less than the bond lengths for the hydrogen-bonded P–O groups of **1–4** ($P–O_{av}$ = 1.484 ± 0.006 Å).

In agreement with the X-ray structures and ^1H NMR data supporting hydrogen bonding in the respective solid and solution states, the broad NH absorptions assigned to the N–H···O modes show lowered frequencies relative to gas-phase imidazole (3518 cm^{-1} [31]).

It is concluded that accurate parameters obtained from X-ray studies for phosphoryl groups hydrogen-bonded to imidazoles and water molecules reported here should prove useful in modeling studies of enzyme–substrate active site interactions.

Experimental Section

The phosphorus acids and heterocyclic nitrogen bases used for the synthesis of hydrogen-bonded imidazolium salts were obtained from Aldrich Chemical Co.

Infrared spectra were taken at ambient temperature with a Perkin-Elmer Model 180 infrared spectrometer. Halocarbon grease mulls were used for taking the spectra in the region between 4000 and 1400 cm^{-1}, and Nujol mulls were used in the region between 1400 and 400 cm^{-1}. The spectrum of liquid 1-methylimidazole was obtained on samples between KBr plates (25 mm in diameter). ^1H NMR spectra were obtained at 22 °C with Varian XL-200 and XL-300 MHz spectrometers. The following solvents were used in the NMR studies: chloroform-*d*, 99.8% deuterated, Cambridge Isotope Laboratory; deuterium oxide, 99.5% deuterated, Baker Chemical Co.; and dimethylsulfoxide-*d*, 99.5% deuterated, Wilmad Corp.

Synthesis of the 1-Methylimidazolium Salt of Diphenyl Phosphate, $[(PhO)_2PO_2][C_3H_3NMeNH]$ (1). 1-Methylimidazole (0.160 mL, 2.01 mmol) was injected into a stirred solution of diphenyl phosphate (0.503 g, 2.01 mmol) in methylene chloride (10 mL) maintained under a nitrogen atmosphere. After 5 h, during which no precipitate formed, diethyl ether was added until it became turbid. On refrigeration overnight, fine crystals were obtained. Recrystallization from hot methylene chloride gave a deliquescent product consisting of fine needles, mp 91.0–92.5 °C (yield 0.603 g, 90%). Anal. Calcd for $C_{16}H_{17}O_4N_2P$: C, 57.83; H, 5.16; N, 8.43; P, 9.32. Found: C, 57.25; H, 5.14; N, 8.37; P, 9.12.

Synthesis of the Imidazolium Salt of Diphenyl Phosphate, $[(PhO)_2PO_2][C_3N_2H_5]$ (2). Diphenyl phosphate (0.505 g, 2.02 mmol) was dissolved in methylene chloride (8 mL). To this solution was added imidazole (0.139 g, 2.04 mmol) with stirring under a nitrogen atmosphere. Stirring was continued for 5 h. Diethyl ether was added to the point of turbidity. Upon refrigeration for 5 days, crystals formed. They were filtered off and dried under vacuum. Recrystallization from a mixture of methylene chloride and Skelly B afforded large crystals, mp 99.0–100.0 °C (yield 0.65 g, 88%). Anal. Calcd for $C_{15}H_{15}O_4N_2P$: C, 56.61; H, 4.75; N, 8.80; P, 9.73. Found: C, 56.23; H, 4.69; N, 8.77; P, 9.47.

Synthesis of the 1-Methylimidazolium Salt of (Trichloromethyl)-phosphonic Acid, $[Cl_3CP(OH)O_2][C_3H_3NMeNH]·H_2O$ (3). To methylene chloride (20 mL) containing undissolved (trichloromethyl)phosphonic acid (2.02 g, 10.1 mmol) was added 1-methylimidazole (0.800 mL, 10.0 mmol) with stirring under a nitrogen atmosphere. A white solid began to form within 5 min. Stirring was continued for 5 h. The solid that formed was filtered off and dried under vacuum. Recrystallization from a warm methanol solution gave the desired product, mp 168.0–169.0 °C (yield 2.08 g, 69%). Anal. Calcd for $C_5H_8O_3N_2Cl_3P$ with one molecule of water: C, 19.98; H, 3.34; N, 9.29; Cl, 35.38; P, 10.23. Found: C, 19.98; H, 3.38; N, 9.36; Cl, 36.71; P, 9.80.

Synthesis of the Imidazolium Salt of (Trichloromethyl)phosphonic Acid, $[Cl_3CP(OH)O_2][C_3N_2H_5]·H_2O$ (4). To (trichloromethyl)phosphonic acid (1.01 g, 5.01 mmol) was added imidazole (0.334 g, 5.05 mmol) dissolved in methylene chloride (20 mL) with stirring under a nitrogen atmosphere. The reaction mixture was stirred for 5 h, after which the solid that formed was filtered off and dried under vacuum. Recrystallization in hot water gave large crystals, which lost their transparency as they were dried under vacuum. This suggested that water molecules were trapped in the crystal lattice which were removed under vacuum, mp 211.5–213.5 °C (yield 1.29 g, 96%). Anal. Calcd for $C_4H_6O_3N_2Cl_3P$: C, 17.96; H, 2.26; N, 10.47; Cl, 39.77; P, 11.58. Found: C, 18.06; H, 2.17; N, 10.47; Cl, 39.93; P, 11.47.

Synthesis of the Imidazolium Salt of Phenylphosphonic Acid, $[PhP(OH)O_2][C_3N_2H_5]$ (5). Into methylene chloride (20 mL) containing phenylphosphonic acid (2.00 g, 12.7 mmol) was added imidazole (0.867 g, 12.7 mmol) with stirring under a dry nitrogen atmosphere. A very viscous material immediately formed. After 5 h of stirring, the viscous material turned to white crystals. They were filtered off and dried under vacuum. Recrystallization from a hot methanol solution afforded a crystalline product, mp 112.0–113.0 °C (yield 2.71 g, 94.6%). Anal. Calcd for $C_9H_{11}O_3N_2P$: C, 47.80; H, 4.90; N, 12.39; P, 13.69. Found: C, 47.66; H, 4.66; N, 12.12; P, 13.43.

Crystallography. All X-ray crystallographic studies were performed with an Enraf-Nonius CAD-4 diffractometer using graphite-monochromated molybdenum radiation ($\lambda K\alpha_1$ = 0.709 30 Å, $K\alpha_2$ = 0.713 59 Å) at an ambient temperature of 23 ± 2 °C. Details of the experimental and computational procedures have been described previously.[32] Crystals were mounted inside thin-walled glass capillaries which were sealed. For **2** and **3**, this procedure was precautionary. For **1** and **4**, it was necessary in order to maintain the integrity of the crystals.

Data were collected by using the θ–2θ scan mode for $2° \le 2\theta_{MoK\alpha} \le 50°$. No corrections were made for absorption. The structures were solved by using a combination of direct methods (MULTAN) and difference Fourier techniques and were refined by using a full-matrix least-squares technique.[33]

X-ray Crystallographic Study for $[(PhO)_2PO_2][C_3H_3NMeNH]$ (1). Crystal data: $C_{16}H_{17}O_4N_2P$, cut from colorless, very hygroscopic square prism needles (0.25 × 0.30 × 0.50 mm), monoclinic space group $P2_1$ [C_2^2-No. 4];[34] a = 7.929 (2) Å, b = 11.353 (3) Å, c = 9.066 (1) Å, β = 103.34 (2)°; Z = 2, $\mu_{MoK\alpha}$ = 0.2012 mm^{-1}; 1478 independent reflections ($+h,+k,\pm l$) measured. The 23 independent non-hydrogen atoms were refined anisotropically, and the 17 hydrogen atoms were refined as isotropic scatterers with B fixed at the next highest integral value of the isotropic temperature factor for the bonded non-hydrogen atom. The final agreement factors[35] were R = 0.027 and R_w = 0.038 for the 1409 reflections having $I \ge 2\sigma_I$.

X-ray Crystallographic Study for $[(PhO)_2PO_2][C_3N_2H_5]$ (2). Crystal data: $C_{15}H_{15}O_4N_2P$, cut from large frosted colorless lathes (0.20 × 0.30 × 0.40 mm), triclinic space group $P\bar{1}$ [C_i^1-No. 2];[36] a = 9.085 (2) Å, b = 9.541 (2) Å, c = 10.473 (2) Å, α = 92.11 (1)°, β = 105.09 (1)°, γ = 115.10 (1)°, Z = 2, $\mu_{MoK\alpha}$ = 0.2007 mm^{-1}; 2750 independent reflections ($+h,\pm k,\pm l$) measured. The 22 independent non-hydrogen atoms were refined anisotropically, and the 15 hydrogen atoms were treated as described for **1**. The final agreement factors[35] were R = 0.044 and R_w = 0.069 for the 2235 reflections having $I \ge 2\sigma_I$.

X-ray Crystallographic Study for $[Cl_3CP(OH)O_2][C_3H_3NMeNH]·H_2O$ (3). Crystal data: $C_5H_8O_3N_2PCl_3·H_2O$, crystal cut from colorless chunky plates (0.28 × 0.30 × 0.43 mm), orthorhombic space group $Pbc2_1$ (alternate setting of $Pca2_1$ [C_{2v}^5-No. 29];[37] a = 8.866 (1) Å, b = 13.510 (2) Å, c = 20.404 (4) Å, Z = 8, $\mu_{MoK\alpha}$ = 0.8741 mm^{-1}; 2207 independent reflections ($+h,+k,+l$) measured. The 30 independent non-hydrogen atoms were refined anisotropically, and the 14 hydrogen atoms were included in the refinement as fixed isotropic scatterers with B fixed at the next highest integral value of the isotropic temperature factor for the bonded non-hydrogen atom. The final agreement factors[35] were R = 0.043 and R_w = 0.060 for the 1840 reflections having $I \ge 2\sigma_I$.

X-ray Crystallographic Study for $[Cl_3CP(OH)O_2][C_3N_2H_5]·H_2O$ (4). Crystal data: $C_4H_6O_3N_2PCl_3·H_2O$, crystal cut from colorless mass of

(31) Bellocq, A. M.; Perchard, C.; Novak, A.; Josien, M. L. *J. Chim. Phys.* **1965**, *62*, 1334.

(32) Sau, A. C.; Day, R. O.; Holmes, R. R. *Inorg. Chem.* **1981**, *20*, 3076.

(33) The function minimized was $\sum w(|F_o| - |F_c|)^2$, where $w^{1/2} = 2F_oLp/\sigma_I$. Mean atomic scattering factors were taken from the following: *International Tables for X-Ray Crystallography*; Kynoch: Birmingham, England, 1974; Vol. IV, pp 72–98. For real and imaginary dispersion corrections for P, Cl and O, see pp 149–150.

(34) *International Tables for X-Ray Crystallography*; Kynoch: Birmingham, England, 1969; Vol. I, p 79.

(35) $R = \sum||F_o| - |F_c||/\sum|F_o|$ and $R_w = \{\sum w(|F_o| - |F_c|)^2/\sum w|F_o|^2\}^{1/2}$. For **1** and **3** these values are for the configuration having the lowest R_w.

(36) Reference 34, p 75.

(37) Reference 34, p 115.

chunks (0.28 × 0.38 × 0.45 mm) which become opaque rapidly in an open container, presumably due to loss of water of hydration, monoclinic space group $P2_1/c$ [C_{2h}^5-No. 14];[38] a = 10.651 (2) Å, b = 6.521 (2) Å, c = 16.277 (4) Å, β = 95.41 (2)°; Z = 4, $\mu_{MoK\alpha}$ = 0.9340 mm^{-1}; 1973 independent reflections ($+h,+k,\pm l$) measured. The 14 independent non-hydrogen atoms were refined anisotropically, and the 18 hydrogen atoms were treated as described for **3**. The final agreement factors[35] were R = 0.048 and R_w = 0.090 for the 1652 reflections having $I \geq 2\sigma_I$.

(38) Reference 34, p 99.

Acknowledgment. The support of this research by the National Science Foundation is gratefully acknowledged.

Supplementary Material Available: Thermal parameters, additional bond lengths and angles, hydrogen atom parameters, atomic coordinates, and refined hydrogen atom parameters for **1-4** (Tables S1-S14) (15 pages). Ordering information is given on any current masthead page.

Chelates as Intermediates in Nucleophilic Additions to Alkoxy Ketones According to Cram's Rule (Cyclic Model)†

Xiangning Chen,‡,∥ Edwin R. Hortelano,‡ Ernest L. Eliel,*,‡ and Stephen V. Frye*,§

Contribution from the Department of Chemistry, University of North Carolina, Chapel Hill, North Carolina 27599-3290, and Glaxo Inc. Research Laboratories, Five Moore Drive, Research Triangle Park, North Carolina 27709. *Received July 1, 1991*

Abstract: Chelates have been considered intermediates in the often highly stereoselective reactions of α-alkoxy and similarly substituted ketones for over 30 years,[10] but without mechanistic evidence. It is now shown, by stop-flow ("rapid injection") NMR kinetics,[15] that the specific rates of reaction of ketones $C_6H_5COCH(OR)CH_3$ with Me_2Mg, where R = $(i\text{-Pr})_3Si$ ("TIPS"), t-$BuPh_2Si$, t-$BuMe_2Si$, Et_3Si, Me_3Si, and Me, parallel the diastereoselectivity of the reaction; i.e., the fastest reacting compound (R = Me) is the one which gives the highest proportion of the product predicted by Cram's chelate rule. The major product of the slowest reacting compound (R = TIPS) is not in accord with Cram's chelate rule, and this compound reacts at the same specific rate as the parent, $C_6H_5COCH_2CH_3$. This is in accord with earlier work indicating that TIPSO does not chelate. Compounds intermediate in the series react at intermediate rates and give the two diastereomeric products in proportions which can be calculated by assuming two competing reactions (cf. Figure 2): one proceeding via the chelated transition states giving the product predicted by the chelate rule and one not involving chelation which gives the same product composition as the R = TIPS compound. Direct steric effects on carbonyl reactivity due to the remote bulky silyloxy substituents have been excluded by the study of carbon analogues bearing similar bulky groups. Thus, the kinetic effect in the above series appears to be due to steric hindrance to chelation; hence, the parallel of specific rate and stereoselectivity demonstrates that high stereoselectivity is associated with strong chelation, as postulated by Cram and Kopecky in 1959.[10]

Introduction

The amazing progress over the last 15 years in the development of enantioselective syntheses has revolutionized the organic chemist's ability to prepare compounds in enantiopure form. However the progress in understanding the mechanistic basis for many of these stereoselective reactions has been much slower. In general, the stereochemical outcome of a particular reaction has led to the proposal of a transition-state model, and thereafter the observation of similar stereochemical results has been taken as evidence for the reaction proceeding via the proposed transition state. Exceptions to the postulated transition-state model simply lead to the proposal of as many competing transition states as necessary to explain the experimental results. While such reasoning is useful, in so far as it allows the extrapolation of results to different substrates or conditions, it is clearly circular and does not necessarily address the mechanism of the reaction in question.

Chelation is often invoked to account for the stereochemical outcome of the reaction between organometallic reagents and substrates containing more than one functional group capable of coordination.[1-10] In acyclic systems, this bidentate interaction between reagent and substrate is proposed to lead to the very high levels of stereoselection often observed. The classical explanation of this phenomenon was presented in 1959 by Cram and Kopecky,[10] who postulated that the steric outcome of additions of organometallic reagents to chiral α-alkoxy ketones rested on the

† Dedicated to Professor Michael Hanack on his 60th birthday.
‡ University of North Carolina.
§ Glaxo Inc.
∥ Glaxo Fellow.

(1) For a review of chelation-controlled reactions of α- and β-alkoxy carbonyl compounds, see: Reetz, M. T. *Angew. Chem., Int. Ed. Engl.* **1984**, *23*, 1035.
(2) Eliel, E. L. In *Asymmetric Synthesis*; Morrison, J. D., Ed.; Academic: New York, 1983; Vol. 2 p 125. Morrison, J. D.; Mosher, H. S. *Asymmetric Organic Reactions*; Prentice-Hall: New York, 1971; Chapter 3.
(3) For some recent examples of stereoselective additions to α-alkoxy aldehydes and ketones rationalized by chelation, see: Martin, S. F.; Li, W. *J. Org. Chem.* **1989**, *54*, 6129. Amouroux, R.; Ejjiyar, S.; Chastrette, M. *Tetrahedron Lett.* **1986**, *27*, 1035. Asami, M.; Kimura, R. *Chem. Lett.* **1985**, 1221. Uenishi, I.-i.; Tomozane, H.; Yamato, M. *J. Chem. Soc., Chem. Commun.* **1985**, 717.
(4) For some recent examples of stereoselective additions to β-alkoxy aldehydes and ketones rationalized by chelation, see: Baldwin, S. W.; McIver, J. M. *Tetrahedron Lett.* **1991**, *32*, 1937. Marshall, J. A.; Wang, X.-j. *J. Org. Chem.* **1990**, *55*, 6246. Tomooka, K.; Okinaga, T.; Suzuki, K.; Tsuchihashi, G.-i. *Tetrahedron Lett.* **1989**, *30*, 1563. Gennari, C.; Cozzi, P. G. *J. Org. Chem.* **1988**, *53*, 4015. Mori, Y.; Kuhara, M.; Takeuchi, A.; Suzuki, M. *Tetrahedron Lett.* **1988**, *29*, 5419.
(5) For some recent examples of stereoselective additions to carbonyl compounds proposed to involve chelation by metal alkoxides, see: Kallmerten, J.; Coutts, S. J. *Tetrahedron Lett.* **1990**, *30*, 4305. Evans, D. A.; Chapman, K. T.; Carreira, E. M. *J. Am. Chem. Soc.* **1988**, *110*, 3560.
(6) Chelation by nitrogen has also been invoked recently: Decamp, A. E.; Kawaguchi, A. T.; Volante, R. P.; Shinkai, I. *Tetrahedron Lett.* **1991**, *32*, 1867. Polt, R.; Peterson, M. A. *Tetrahedron Lett.* **1990**, *31*, 4985. Mikami, K.; Kaneko, M.; Loh, T.-P.; Terada, M.; Nakai, T. *Tetrahedron Lett.* **1990**, *31*, 3909. Prasad, V.; Rich, D. H. *Tetrahedron Lett.* **1990**, *31*, 1803. For a structural investigation of nitrogen chelation, see also: Arnett, E. M.; Nichols, M. A.; McPhail, A. T. *J. Am. Chem. Soc.* **1990**, *112*, 7059. See also ref 9b.

0002-7863/92/1514-1778$03.00/0 © 1992 American Chemical Society